Cell Death and Differentiation (2013) 20, 1230–1240

www.nature.com/cdd

Milk fat globule-EGF factor 8 mediates the enhancement of apoptotic cell clearance by glucocorticoids

K Lauber*[,1,2], H Keppeler[1], LE Munoz[3], U Koppe[1], K Schröder[3], H Yamaguchi[4], G Krönke[3], S Uderhardt[3], S Wesselborg[1,5], C Belka[2], S Nagata[4] and M Herrmann[3]

The phagocytic clearance of apoptotic cells is essential to prevent chronic inflammation and autoimmunity. The phosphatidylserine-binding protein milk fat globule-EGF factor 8 (MFG-E8) is a major opsonin for apoptotic cells, and MFG-E8$^{-/-}$ mice spontaneously develop a lupus-like disease. Similar to human systemic lupus erythematosus (SLE), the murine disease is associated with an impaired clearance of apoptotic cells. SLE is routinely treated with glucocorticoids (GCs), whose anti-inflammatory effects are consentaneously attributed to the transrepression of pro-inflammatory cytokines. Here, we show that the GC-mediated transactivation of MFG-E8 expression and the concomitantly enhanced elimination of apoptotic cells constitute a novel aspect in this context. Patients with chronic inflammation receiving high-dose prednisone therapy displayed substantially increased MFG-E8 mRNA levels in circulating monocytes. MFG-E8 induction was dependent on the GC receptor and several GC response elements within the MFG-E8 promoter. Most intriguingly, the inhibition of MFG-E8 induction by RNA interference or genetic knockout strongly reduced or completely abolished the phagocytosis-enhancing effect of GCs *in vitro* and *in vivo*. Thus, MFG-E8-dependent promotion of apoptotic cell clearance is a novel anti-inflammatory facet of GC treatment and renders MFG-E8 a prospective target for future therapeutic interventions in SLE.
Cell Death and Differentiation (2013) **20**, 1230–1240; doi:10.1038/cdd.2013.82; published online 5 July 2013

The elimination of apoptotic cells is fundamentally important for the maintenance of tissue homeostasis in multicellular organisms.[1–3] It prevents the onset of secondary necrosis and the concomitant leakage of cytotoxic and autoantigenic intracellular contents, which potently can trigger tissue damage, chronic inflammation and autoimmunity.[4,5] For their timely removal, apoptotic cells expose several 'eat-me' signals, including phosphatidylserine (PS), on their cell surface. PS, in turn, is recognized either directly by various phagocyte receptors, such as TIM-1, −3, −4, BAI-1 and stabilin-2,[6–9] or indirectly by opsonizing bridging proteins and their corresponding receptors.[10,11] Milk fat globule-EGF factor 8 (MFG-E8), which bridges externalized PS on the apoptotic cell surface to $\alpha_v\beta_3$ or $\alpha_v\beta_5$ integrins on the phagocyte, has a central role in this scenario.[12–15] MFG-E8$^{-/-}$ mice exhibit an autoimmune phenotype closely resembling human systemic lupus erythematosus (SLE), which is characterized by a profound enlargement of lymphoid organs, the appearance of anti-nuclear and anti-dsDNA autoantibodies, deposition of immune complexes in the kidney and consecutively glomerulonephritis.[16,17] In addition, there is accumulating evidence that human SLE is associated with impaired apoptotic cell clearance.[5,18] A standard treatment for chronic inflammatory diseases, like SLE, is the application of glucocorticoids (GCs), whose broad-range anti-inflammatory effects largely are currently attributed to a general transrepression of pro-inflammatory cytokines by interfering with the activity of diverse transcription factors, including NF-κB.[19] However, systemic GC treatment is accompanied by many adverse side effects, including insulin resistance, osteoporosis, glaucoma, skin atrophy or disturbed wound healing, which often limit GC applicability in the long run.[20] Consequently, novel and molecularly targeted therapies for chronic inflammatory and autoimmune diseases are urgently required.

Here, we present a novel aspect of GC-mediated anti-inflammation. We show that GC-dependent transactivation of MFG-E8 expression enhances the clearance of apoptotic cells. Our results reveal a strong positive correlation between high-dose prednisone therapy and MFG-E8 mRNA expression in peripheral blood monocytes of patients with chronic inflammation. *In vitro* application of dexamethasone (Dex) resulted in a profound induction of MFG-E8 expression on mRNA as well as on protein level. This was specifically observed in certain myeloid cells and was dependent on the

[1]Department of Internal Medicine I, University of Tuebingen, Tuebingen, Germany; [2]Department of Radiation Oncology, LMU Munich, Ludwig-Maximilians-University, Munich, Germany; [3]Department of Internal Medicine 3, Friedrich-Alexander University, Erlangen, Germany; [4]Department of Medical Chemistry, Graduate School of Medicine, Kyoto University, Kyoto, Japan and [5]Institute for Molecular Medicine, Heinrich-Heine-University, Duesseldorf, Germany
*Corresponding author: K Lauber, Department of Radiation Oncology, LMU Munich, Ludwig-Maximilians-University, Marchioninistr. 15, Munich 81377, Germany. Tel: +49 89 7095 6740; Fax: +49 89 7095 6770; E-mail: kirsten.lauber@med.uni-muenchen.de
Keywords: apoptotic cell clearance; MFG-E8; phagocytosis; glucocorticoids; autoimmunity
Abbreviations: ActD, actinomycin D; Anx A1, annexin A1; ARE, AU-rich element; CHX, cycloheximide; Del-1, developmental endothelial locus-1; Dex, dexamethasone; GC, glucocorticoid; GR, GC receptor; GRE, GC response element; MerTK, Mer tyrosine kinase; MFG-E8, milk fat globule-EGF factor 8; PS, phosphatidylserine; qRT-PCR, quantitative real-time RT-PCR; SEGRA, selective GR agonist; UTR, untranslated region
Received 11.12.12; revised 29.5.13; accepted 30.5.13; Edited by H-U Simon; published online 05.7.13

GC receptor (GR), as well as several GC response elements (GREs) within the MFG-E8 promoter. Macrophages, which had been treated with Dex, displayed a substantially enhanced capacity to engulf apoptotic cells but not synthetic microspheres or fragments of secondary necrotic cells. Importantly, the phagocytosis-enhancing effect of Dex was strongly reduced or completely abolished by inhibition of MFG-E8 induction by RNA interference or genetic knockout *in vitro* and in a mouse model of irradiation-induced thymus atrophy.

In conclusion, our study identifies MFG-E8-dependent promotion of apoptotic cell clearance as a novel anti-inflammatory aspect of GC treatment and renders MFG-E8, as well as the regulation of its expression in myeloid cell subsets, prospective targets for future therapeutic interventions in chronic inflammatory diseases.

Results

GC treatment leads to upregulation of MFG-E8 expression in certain myeloid cells. MFG-E8 is a crucial engulfment factor in the phagocytic synapse of apoptotic cell clearance—a process whose defects are well-known to be associated with chronic inflammation and autoimmunity in SLE.[4,5,12,16,18] The present study was designed to examine whether monocytes of patients with chronic inflammatory disorders display reduced expression levels of MFG-E8. To this end, we measured MFG-E8 expression in peripheral blood monocytes of normal healthy donors and patients with chronic inflammatory rheumatic diseases (rheumatoid arthritis, SLE, dermatomyositis and Sjögren's syndrome, for patients' data see Supplementary Table 1) by quantitative real-time RT-PCR (qRT-PCR). We did not detect a significant reduction in MFG-E8 mRNA levels in any of the patients' samples (Figure 1a). Instead, we observed that some of the patients' samples displayed profoundly increased MFG-E8 mRNA levels. Careful analysis of the clinical records revealed that six out of seven patients, who were receiving more than 35 mg/week prednisone, exhibited an elevated expression of MFG-E8 mRNA (Figure 1b). It should be noted that this clear-cut association between high-dose prednisone administration and increased mRNA expression was exclusively observed for MFG-E8 and not for the other engulfment-related genes tested (Supplementary Table 2).

The close association between high-dose prednisone treatment and increased MFG-E8 mRNA levels (Figure 1b) strongly suggested that GC treatment might be causative for the upregulation of MFG-E8 expression. When we stimulated differentiated THP-1 macrophages with Dex *in vitro*, we observed a dose-dependent induction of MFG-E8 expression on mRNA, as well as on protein level (Figure 1c). No such effect was seen with the close MFG-E8 relative developmental endothelial locus-1 (Del-1)[21] or the known GC-inducible gene annexin A1 (Anx A1).[22] Interestingly, the majority of MFG-E8 remained associated with the macrophages as confirmed by ELISA measurements of cellular lysates and cell-free culture supernatants (Figure 1e). Most likely, immediately upon its secretion MFG-E8 binds to $\alpha_v\beta_{3/5}$ integrins, which are abundantly expressed on the macrophage cell surface. Similar findings (cell-association of newly synthesized MFG-E8 upon GM-CSF-dependent induction) were reported by Jinushi *et al.*[23] Kinetic analyses revealed that the Dex-mediated induction of MFG-E8 expression in THP-1 macrophages was rather slow, becoming measurable on mRNA and protein level at $\sim$4 h and 8 h after stimulation, respectively. Maximal induction was detected after 24 h (Figure 1d). Again, no or only a marginal, transient induction of Anx A1 or Del-1 mRNA expression was observed. Most importantly, the Dex-dependent upregulation of MFG-E8 expression was specific for certain subsets of myeloid cells, as it was only detected in primary monocytes, the monocytic cell lines THP-1, U937 and Mono Mac 6, and macrophages derived thereof, but not in primary human foreskin fibroblasts, murine NIH3T3 fibroblasts or phytohemagglutin (PHA)-stimulated lymphoblasts (Figure 1f). For comparison, we also analyzed the mRNA expression of $\alpha_v\beta_3$ integrins in these cells but did not detect an upregulation in response to Dex treatment as in case of MFG-E8 (Supplementary Figures 1A and B).

GC treatment specifically promotes the engulfment of apoptotic cells by macrophages. Previous studies had shown that GC treatment of macrophages results in enhanced phagocytic uptake of apoptotic cells.[24] However, the underlying molecular mechanisms largely remained elusive. Next, we therefore examined whether GC application generally improves the phagocytic capacity or if the enhanced engulfment is specific for apoptotic cells. To this end, we fed control or Dex-treated THP-1 macrophages with different classes of phagocytic prey: apoptotic cells, 6 μm microspheres and fragments of secondary necrotic cells. Interestingly, Dex treatment only promoted the phagocytosis of apoptotic prey (Figure 2a) suggesting that Dex specifically enhances the internalization of apoptotic cells (most likely as a result of improved recognition) and not the process of phagocytosis in general.

Dose–response analyses revealed that the phagocytosis-enhancing effect of Dex paralleled the induction of MFG-E8 protein expression. Both became traceable in the presence of 1 nM Dex reaching a saturation level at $\sim$100 nM Dex (Figure 2b). Both followed a similar kinetics becoming detectable around 8 h and attaining a maximum $\sim$24 h after stimulation (Figure 2c), and again, the Dex-dependent enhancement of phagocytosis was specifically observed for apoptotic cells, but not for 6 μm microspheres or fragments of secondary necrotic cells, respectively.

In order to extend our experiments to other macrophage populations, primary human macrophages obtained from peripheral blood monocytes by differentiation in the presence of M-CSF or GM-CSF, as well as differentiated U937 macrophages, were employed. All of them confirmed the Dex-dependent promotion of apoptotic cell engulfment (Figures 2d and e and Supplementary Figures 2A and B). In contrast, no comparable effect was observed with murine NIH3T3 fibroblasts expressing the MFG-E8 receptor $\alpha_v\beta_3$ integrin (Supplementary Figure 2C). These cells were capable of phagocytosing apoptotic neutrophils when purified MFG-E8 was applied exogenously (Supplementary Figure 2C), but they failed to upregulate endogenous MFG-E8 expression in

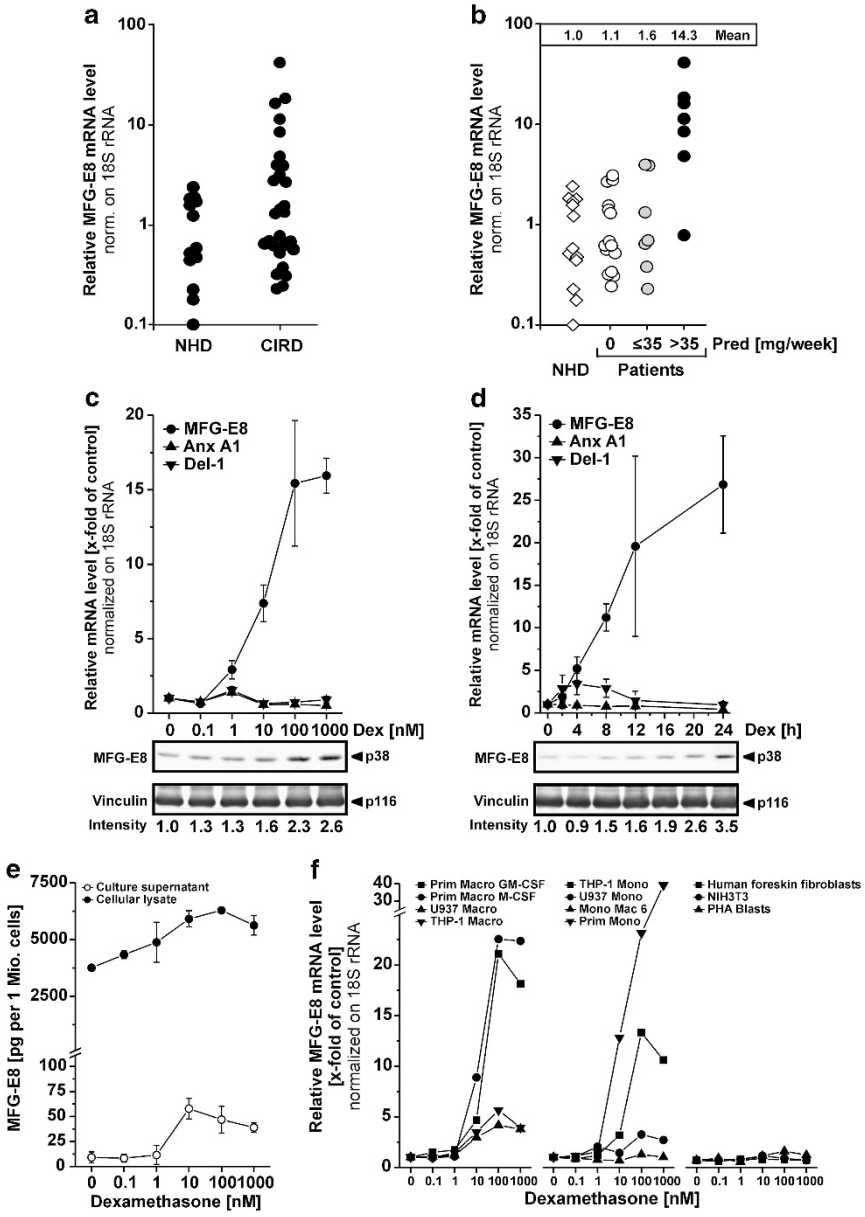

Figure 1 Enhanced expression by certain myeloid cells of MFG-E8 in response to treatment with glucocorticoids. (**a**) MFG-E8 mRNA expression was examined in peripheral blood monocytes from normal healthy donors (NHD, $n = 13$) and patients with chronic inflammatory rheumatic diseases (CIRD, $n = 29$) by qRT-PCR. The relative mRNA levels were normalized on 18S rRNA and calibrated on the mean value of the NHD population. (**b**) Results from (**a**) plotted against the weekly dose of prednisone (Pred) the patients were receiving. $n = 13$ for NHD, $n = 15$ for CIRD patients with 0 mg/week Pred, $n = 7$ for CIRD patients with ≤ 35 mg/week Pred and $n = 7$ for CIRD patients with > 35 mg/week Pred. (**c**) PMA-differentiated THP-1 macrophages were treated with dexamethasone (Dex) for 24 h. MFG-E8 expression was examined on mRNA level by qRT-PCR and protein level by non-reducing SDS-PAGE with subsequent immunoblot analysis (loading control vinculin). The relative mRNA levels were normalized on 18S rRNA and calibrated on the untreated control population (means ± S.D. from triplicates from one representative out of two experiments). Relative mRNA levels of Annexin A1 (Anx A1) and developmental endothelial locus-1 (Del-1) were measured as controls. (**d**) THP-1 macrophages were treated with 1 μM Dex for 0–24 h. MFG-E8 expression was examined on mRNA and protein level as in (**c**) (means ± S.D. from triplicates from one representative out of two experiments). (**e**) MFG-E8 protein levels were quantified in culture supernatants and cellular lysates of dexamethasone-treated THP-1 macrophages treated as in (**c**) by ELISA. Means ± s.d. of triplicates are depicted. (**f**) Primary human monocytes, monocytic cells lines, monocyte-derived primary human macrophages, macrophages differentiated from THP-1 or U937 cells, human foreskin fibroblasts, murine NIH3T3 fibroblasts and PHA-stimulated human lymphoblasts were treated with dexamethasone (Dex) for 24 h and MFG-E8 expression was examined on mRNA level by qRT-PCR as in (**c**). Mean values of duplicates from one representative out of 3 experiments are shown

the presence of Dex – apparently because they are not of myeloid origin (Figure 1e).

Two recent studies provided evidence for the Dex-dependent upregulation of Mer tyrosine kinase (MerTK) and for the involvement of the serum-derived opsonin Protein S in GC-mediated enhancement of apoptotic cell engulfment.[25,26] Next, we therefore compared the phagocytosis of apoptotic cells in the presence and absence of serum, and observed a Dex-dependent increase in the presence of serum confirming the results from McColl *et al.*[25] and Zahuczky *et al.*[26]

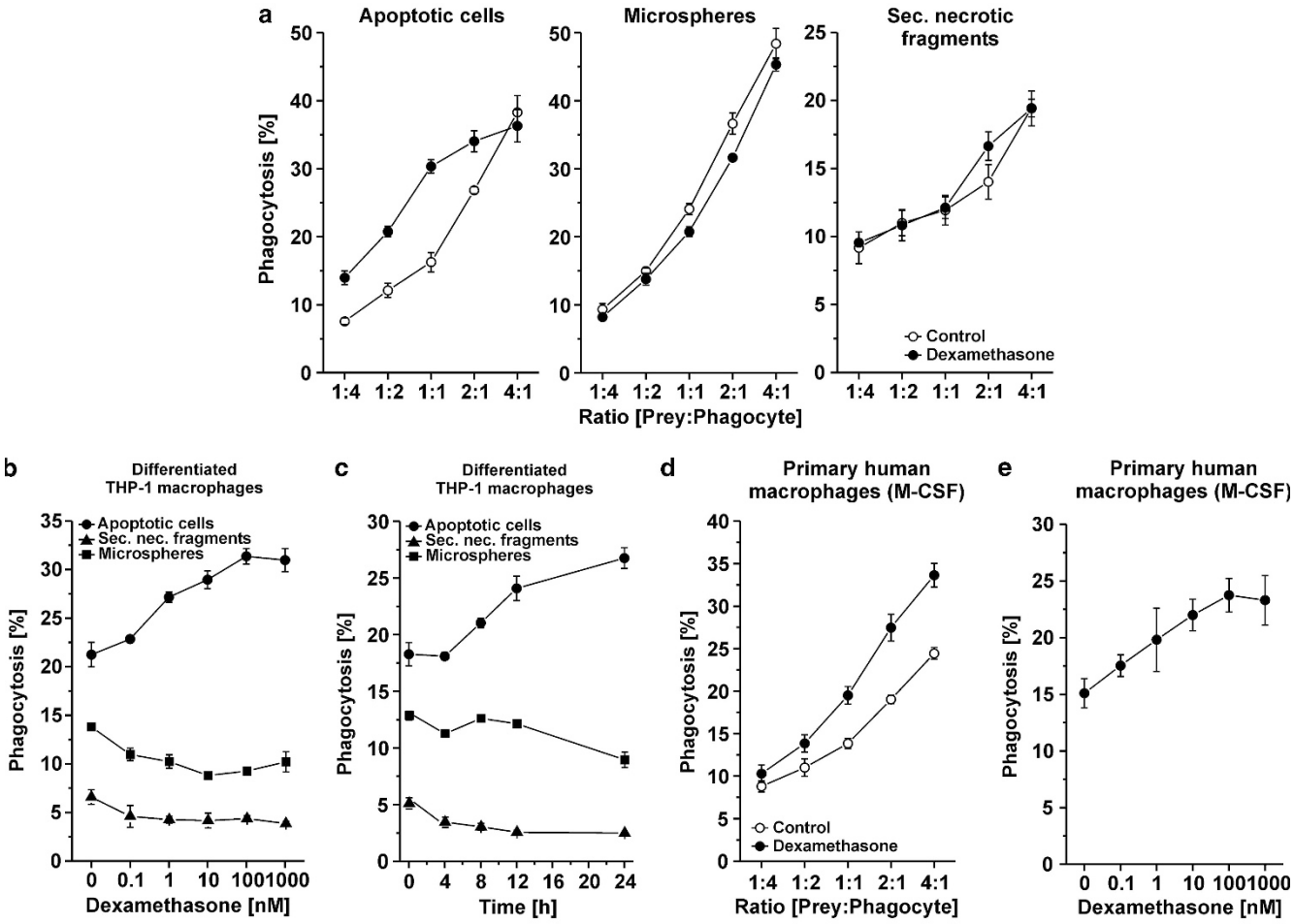

Figure 2 Dexamethasone treatment dose- and time-dependently leads to enhanced uptake of apoptotic cells by macrophages. (**a**) PMA-differentiated THP-1 macrophages were treated with or without 1 μM Dex for 24 h and subsequently were fed with different ratios of apoptotic THP-1 cells, 6 μm microspheres or secondary necrotic fragments. After 2 h of incubation, phagocytosis was assessed flow cytometrically and is given as percentage of macrophages with ingested material (means ± S.D. from quadruplicates from one representative out of three experiments). (**b**) THP-1 macrophages were treated with Dex for 24 h and subsequently applied to a phagocytosis assay with a ratio of 1 : 1 apoptotic THP-1 cells, 6 μm microspheres or secondary necrotic fragments, respectively. Phagocytosis was assessed as in (**a**) (means ± S.D. from quadruplicates from one representative out of three experiments). (**c**) THP-1 macrophages were treated with 1 μM Dex for 0–24 h. Uptake of apoptotic THP-1 cells (ratio 1 : 1) was measured as in (**a**) (means ± S.D. from quadruplicates from one representative out of three experiments). (**d**) Primary human macrophages differentiated with M-CSF from peripheral blood monocytes were treated with or without 1 μM Dex for 24 h and applied to a phagocytosis assay with autologous apoptotic neutrophils as in (**a**). Means ± S.D. from quadruplicates from one representative out of two experiments are shown. (**e**) Primary human monocyte-derived macrophages were treated with Dex for 24 h and phagocytosis of autologous apoptotic neutrophils (ratio 1 : 2) was determined as in (**b**) (means ± S.D. from quadruplicates from one representative out of two experiments)

However, the Dex-mediated enhancement of apoptotic cell ingestion in the absence of serum apparently derives from a serum-independent engulfment system, such as MFG-E8 and the corresponding phagocyte receptor $\alpha_v\beta_{3/5}$ integrin (Supplementary Figure 2D).

GC treatment leads to direct, GR-dependent transactivation of MFG-E8 expression via various GREs in the MFG-E8 promoter and prolongs MFG-E8 mRNA stability. Next, we elucidated the molecular mechanisms of GC-dependent MFG-E8 induction in further detail. GCs are known to enhance target gene expression either directly via GR-controlled *cis*-acting GREs or indirectly via the GR-dependent induction of additional transcription factors, which subsequently drive target gene expression in *trans*.[19] *In silico* promoter analyses of the 1 kb region upstream of the transcription start site disclosed several full- and half-site GRE consensus motifs within the human MFG-E8 promoter (Figure 3a). Hence, it was conceivable that GC-mediated MFG-E8 induction was directly regulated via GR-dependent transactivation at the GREs. This hypothesis was confirmed by qRT-PCR analyses of THP-1 macrophages, which had been treated with Dex in the presence or absence of the GR antagonist RU486 or the protein synthesis inhibitor cycloheximide (CHX) (Figures 3b and c). RU486 completely abrogated MFG-E8 induction in response to treatment with Dex, whereas CHX was not inhibitory. Thus, the GR but no *de novo* synthesized, additional transcriptional regulator was required for Dex-dependent induction of MFG-E8 expression. To identify the GREs essentially involved in the

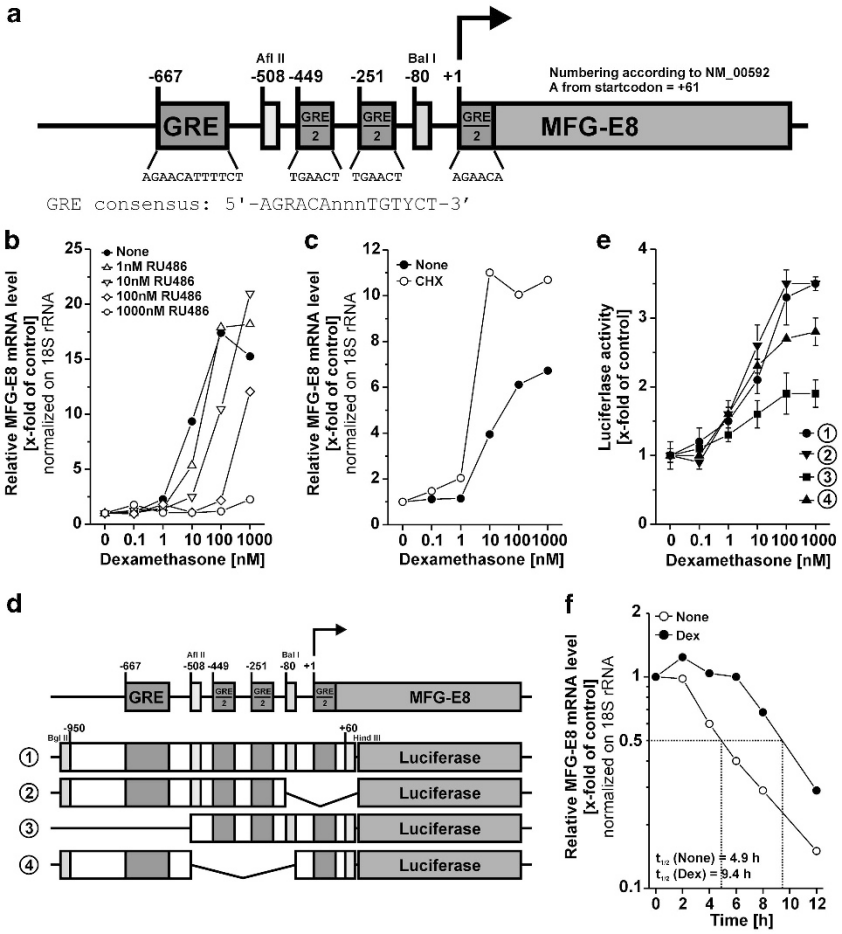

Figure 3 Different GREs in the promoter region of human MFG-E8 are required for dexamethasone-dependent MFG-E8 expression. (**a**) Schematic map of putative GREs within the minus 1000-bp region of the human MFG-E8 promoter. Positions of GREs and restriction sites are numbered according to NM_00592. (**b**) THP-1 macrophages were treated with Dex in the presence or absence of 10 μM RU486 for 24 h. MFG-E8 mRNA levels were quantified by qRT-PCR as in Figure 1c (means of duplicates from one representative out of two experiments). (**c**) THP-1 macrophages were treated with Dex in the presence or absence of 10 μg/ml of cycloheximide (CHX) for 24 h. MFG-E8 mRNA levels were assessed as in Figure 1c (mean values of duplicates from one representative out of two experiments). (**d**) Schematic map of the MFG-E8 promoter constructs employed in (**e**). (**e**) Different regions of the human MFG-E8 promoter cloned into pGL3 Basic (see (**d**)) were lipofected into THP-1 macrophages for 5 h and subsequently cells were treated with Dex for 16 h. Luciferase activities were measured in cellular lysates and calibrated on the corresponding untreated control populations (mean values ± S.D. of triplicates from one representative out of three experiments). (**f**) THP-1 macrophages were treated with or without 1 μM Dex for 2 h before RNA synthesis inhibition with 100 ng/ml actinomycin D. The decay of MFG-E8 mRNA was measured by qRT-PCR. Half-lives ($t_{1/2}$) of MFG-E8 mRNA were determined and are depicted in the plot (means of duplicates from one representative out of two experiments)

transactivation process, we tested several luciferase reporter constructs comprising various parts of the 1 kb region of the human MFG-E8 promoter (Figure 3e) for their Dex responsiveness in reporter assays (Figure 3d). We observed the strongest Dex-dependent induction with the constructs containing all of the predicted GREs or lacking only the putative GRE half-site at position +1. The deletion mutant deficient in the predicted GRE half-sites at -449 and -251 displayed a slightly decreased Dex responsiveness and the construct lacking the full GRE at -667 showed the weakest response. Hence, we conclude that the Dex-dependent induction of MFG-E8 expression was mainly driven by the GRE at -667 with minor contribution of the two GRE half-sites at -449 and -251.

Apart from their effects on transcription, GCs modulate target gene expression on the post-transcriptional level, particularly by controlling mRNA stability.[27] To clarify whether this also applies to MFG-E8, we measured the decay of MFG-E8 mRNA in the presence or absence of Dex after inhibition of transcription by actinomycin D (ActD). We observed a Dex-dependent stabilizing effect resulting in a nearly twofold prolonged half-life of the MFG-E8 mRNA (Figure 3f).

GC-dependent transactivation of MFG-E8 expression is crucial for the promotion of apoptotic cell clearance. To address the crucial question whether the induction of MFG-E8 expression is responsible for the Dex-dependent enhancement of apoptotic cell engulfment by macrophages, we inhibited MFG-E8 induction by RNA interference. Transfection with the MFG-E8-specific siRNA resulted in reduced Dex-mediated promotion of phagocytosis in comparison with the scrambled control oligonucleotide in THP-1 macrophages, as well as in primary M-CSF-differentiated macrophages (Figure 4a; Supplementary Figure 3A).

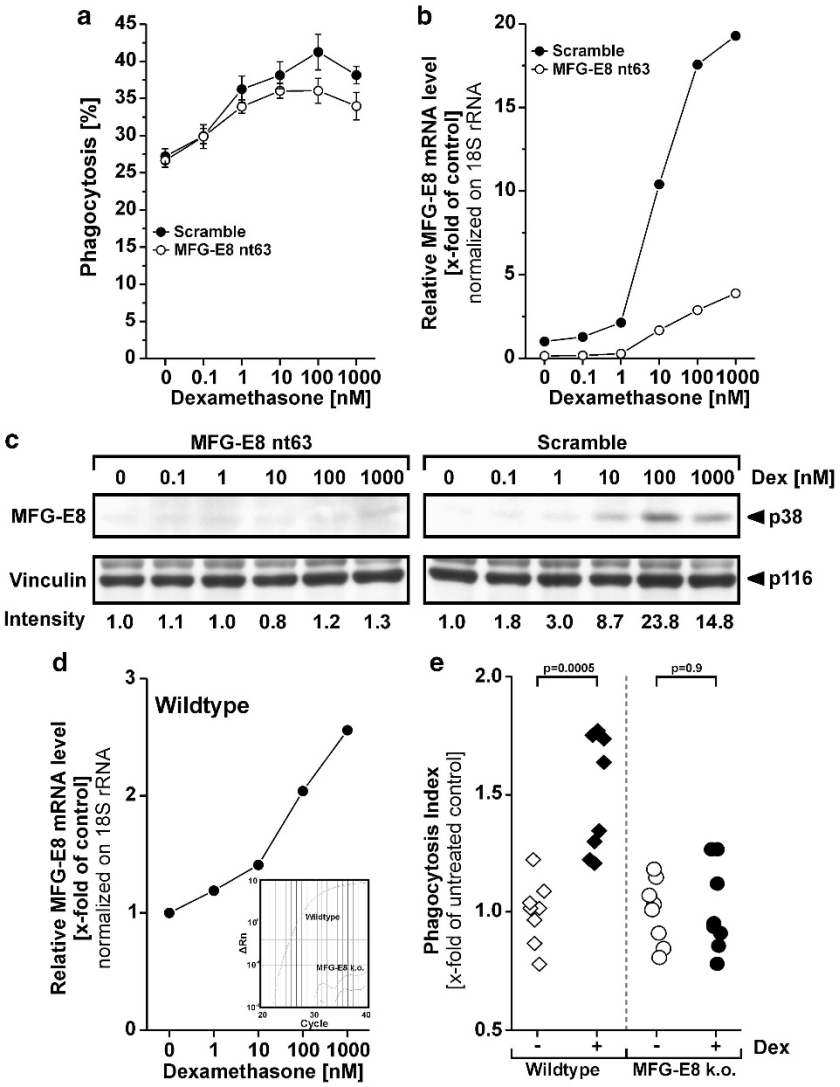

Figure 4 Inhibition of MFG-E8 expression by RNA interference or genetic knockout results in reduced phagocytosis promotion by dexamethasone treatment. (**a**) THP-1 monocytes were electroporated with an MFG-E8-specific siRNA oligonucleotide or the corresponding scrambled sequence before being differentiated into macrophages and treatment with Dex for 24 h. Phagocytosis of apoptotic prey cells was measured as in Figure 2b (means ± S.D. from quadruplicates from one representative out of two experiments). (**b**) MFG-E8 knockdown, macrophage differentiation and Dex treatment of THP-1 cells were carried out as in (**a**) and MFG-E8 mRNA expression was assessed by qRT-PCR. Relative mRNA levels were normalized on 18S rRNA and calibrated on the untreated scramble-transfected control population (means of duplicates from one representative out of two experiments). (**c**) MFG-E8 knockdown, macrophage differentiation and Dex treatment of THP-1 cells were carried out as in (**a**) and MFG-E8 protein expression was detected by immunoblot analysis as in Figure 1c (one representative out of two experiments). (**d**) Thioglycollate-elicited peritoneal macrophages were prepared from wild-type and MFG-E8-knockout mice. *In vitro* macrophages were treated with 500 nM Dex for 24 h before quantitation of MFG-E8 mRNA by qRT-PCR (means of duplicates). In MFG-E8$^{-/-}$ cells, no MFG-E8 mRNA was detected. The inlay shows examples of the primary amplification curves. (**e**) Macrophages were prepared and treated as in (**d**). Subsequently, phagocytosis of apoptotic third-party thymocytes was measured and is depicted as phagocytic index (percentage of macrophages with ingested material × mean of internalized prey cell fluorescence) normalized on the corresponding untreated control population ($n = 8$). *P*-values were calculated by heteroskedastic, unpaired, two-tailed Student's *t*-test analysis

However, a residual phagocytosis-enhancing effect of Dex treatment was still detected in MFG-E8-knockdown cells. This might be owing to the fact that MFG-E8 induction on mRNA, as well as on protein level, was clearly reduced but not completely blocked (Figures 4b and c; Supplementary Figure 3B). Therefore, we analyzed the effect of Dex treatment on the phagocytosis of apoptotic thymocytes by thioglycollate-elicited macrophages of MFG-E8$^{-/-}$ or wild-type C57BL/6 mice, respectively. A clear Dex-mediated enhancement of apoptotic cell phagocytosis was measurable in the wild-type macrophages (Figure 4e) even though the Dex-dependent induction of MFG-E8 mRNA was not as intense as in the human system (Figure 4d). Most importantly, the Dex-dependent promotion of phagocytosis was completely absent in the MFG-E8$^{-/-}$ macrophages, which – as to be expected – did not express any detectable MFG-E8 mRNA at all.

Finally, we employed a mouse model of irradiation-induced thymus atrophy in order to evaluate our findings *in vivo.* Wild-type C57BL/6 mice or MFG-E8$^{-/-}$ mice were treated with

1 mg/kg/week Dex intraperitoneally for 1 week. Then, in order to induce thymocyte apoptosis, mice were irradiated with 0.5 Gy, and thymus atrophy was determined on the basis of the residual thymus mass as percentage of the non-irradiated controls (Figures 5a and b). At 8 h after irradiation, the thymus weight decreased in average to 80% (wild type) or 87% (MFG-E8$^{-/-}$) of the non-irradiated controls, respectively, with no significant difference between wild-type and MFG-E8$^{-/-}$ animals ($P = 0.49$). Importantly, wild-type mice that had been pre-treated with Dex for 1 week revealed a significant acceleration of thymus atrophy (mean residual thymus mass 8 h after irradiation, 66%), which was not

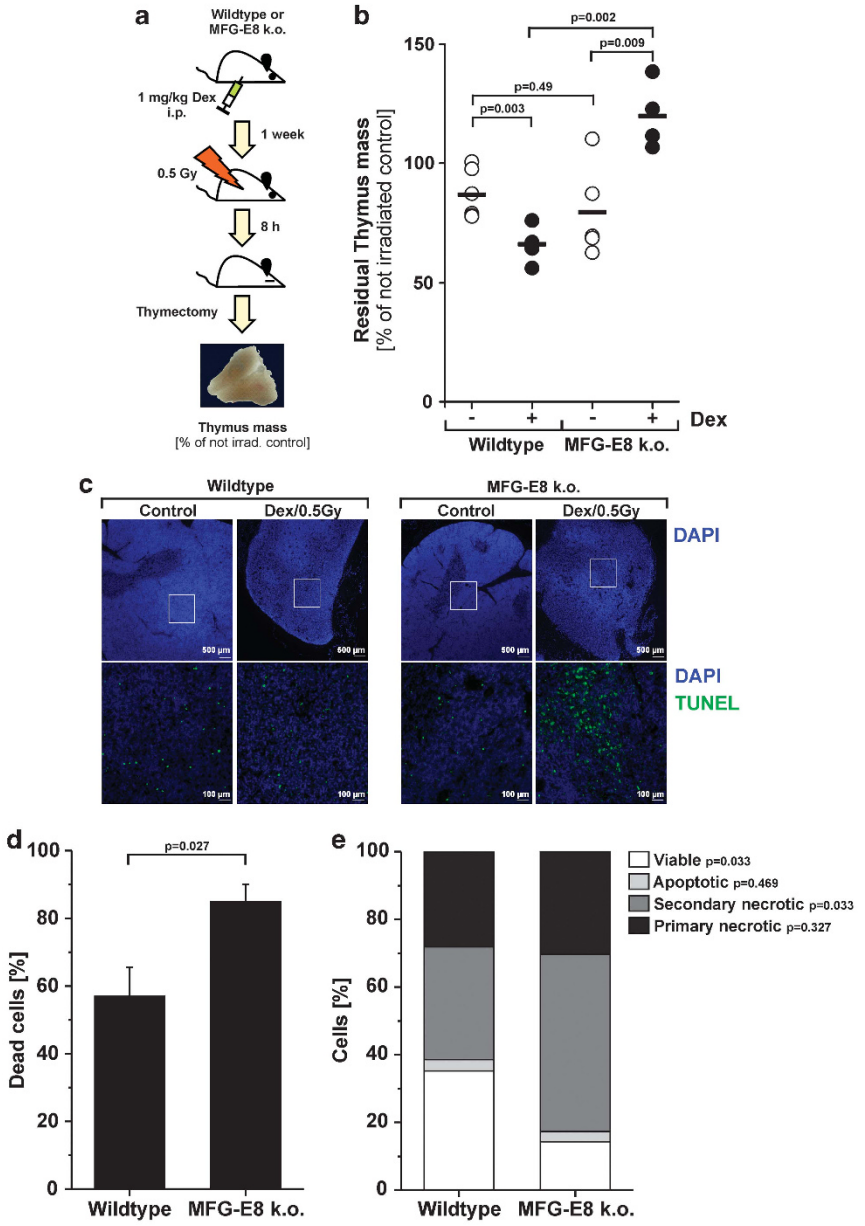

Figure 5 Dex-induced acceleration of irradiation-induced thymus atrophy is dependent on MFG-E8. (**a**) Schematic of the experimental setup. (**b**) C57BL/6 and MFG-E8$^{-/-}$ mice were treated with 1mg/kg/week Dex i.p. (for C57BL/6 $n = 6$, for MFG-E8$^{-/-}$ $n = 4$) or vehicle (for C57BL/6 $n = 6$, for MFG-E8$^{-/-}$ $n = 5$) for 1 week (Dex was applied in seven daily doses). Then, mice were irradiated with 0.5 Gy, killed after 8 h and thymi were excised. Thymus atrophy was measured as percentage of thymus weight in comparison with non-irradiated controls. Open and closed circles represent the values obtained for individual animals and bars indicate the means. *P*-values were calculated by heteroskedastic, unpaired, two-tailed Student's *t*-test analysis. (**c**) Paraffin sections of explanted thymi of Dex-treated, irradiated C57BL/6 and MFG-E8$^{-/-}$ mice were subjected to TUNEL–FITC staining for dying cells with DNA strand breaks and DAPI for total nuclei. Pictures were taken at $\times 2$ (upper panel) or $\times 10$ magnification (lower panel), respectively. (**d**) Explanted thymi of Dex-treated, irradiated C57BL/6 and MFG-E8$^{-/-}$ mice were mechanically disrupted, and flushed-out, collected cells were analyzed by FSC/SSC flow cytometry. The percentage of dead cells was determined from the percentage of cells with low FSC and high SSC. Means + S.E. are shown and *P*-value was calculated by heteroskedastic, unpaired, two-tailed Student's *t*-test analysis. (**e**) Collected cells from mechanically disrupted and flushed-out thymi of Dex-treated, irradiated C57BL/6 and MFG-E8$^{-/-}$ mice as prepared in (**d**) were subjected to 6-parameter FACS analyses. Different types of dead cells were classified as described in Materials and Methods. *P*-values were calculated by heteroskedastic, unpaired, two-tailed Student's *t*-test analysis

detectable in MFG-E8$^{-/-}$ animals. Here, even a slight increase in thymus mass was observed (mean residual thymus mass 8 h after irradiation, 120%). Histological examinations revealed a profound disintegration of thymus architecture in Dex-treated, irradiated wild -type, as well as MFG-E8$^{-/-}$, animals. However, a striking accumulation of TUNEL-positive, dying cells was only observed in MFG-E8$^{-/-}$ mice (Figure 5c). In order to quantify this in further detail, explanted thymi of Dex-treated, irradiated animals were mechanically disrupted, and the flushed-out, liberated cells were subjected to FSC/SSC FACS analyses. We observed a significant accumulation of dead cells with low FSC and high SSC in the preparations of MFG-E8$^{-/-}$ thymi compared with the wild-type controls (Figure 5d). Further subclassification by 6-parameter FACS staining revealed that this was basically due to an accumulation of secondary necrotic cells, which obviously had not been efficiently engulfed in MFG-E8$^{-/-}$ thymi (Figure 5e). Of note, these differences were not owing to differences in thymocyte apoptosis, as *in vitro* irradiation-induced cell death (apoptosis as well as necrosis) of wild-type and MFG-E8$^{-/-}$ thymocytes displayed parallel kinetics, dose-dependency and extent (Supplementary Figure 4). Moreover, the low-dose Dex treatment over 1 week did not induce significant thymus atrophy before irradiation. Hence, our results support a scenario, in which Dex treatment and the subsequent upregulation of MFG-E8 expression accelerate thymus atrophy by an increased clearance of apoptotic thymocytes.

Discussion

For more than 50 years, GCs, like cortisone, Dex and prednisone, have been among the most effective and widely used medications for the treatment of inflammatory diseases, some of these reportedly associated with delays and defects in apoptotic cell clearance.[4,5,18,28] To date, the anti-phlogistic effects of GCs principally are considered to be caused by GR-mediated transrepression of pro-inflammatory cytokines.[19] Here, we describe a novel anti-inflammatory function of GCs: the enhancement of apoptotic cell removal by direct, GR-dependent induction of MFG-E8 expression.

Although the first report on GC-mediated promotion of apoptotic cell engulfment was published more than a decade ago,[24] the underlying molecular mechanisms remained obscure. So far, a general enhancement of the phagocytic capability owing to decreased p139Cas expression and concomitantly accelerated cytoskeletal rearrangements had been suggested as molecular explanations.[29] However, our results do not support this hypothesis, as Dex treatment specifically enhanced the internalization of apoptotic cells but not synthetic microspheres or fragments of secondary necrotic cells. Alternatively, Maderna *et al.*[30] had proposed that an increased expression of Anx A1, another bridging protein in the phagocytic synapse, might contribute to the Dex-dependent enhancement of apoptotic cell removal. In our cell system, consistent with previous reports,[31,32] we did not observe a Dex-dependent induction of Anx A1 expression. Hence, this is unlikely to be causative for the phagocytosis-promoting effect examined in the present study. Intriguingly, the unambiguous association between high-dose prednisone administration and increased mRNA expression in peripheral monocytes was only observed in case of MFG-E8 but not for the other genes of the phagocytic synapse tested. This confers a unique characteristic to MFG-E8 among the known engulfment-related genes – especially in view of the fact that GCs are known to modulate the expression of 10–15% of all human genes.[27]

Two recent studies have shown that serum factors and particularly protein S are involved in Dex-dependent promotion of apoptotic cell phagocytosis.[25,26] Protein S is a PS-binding serum protein, which opsonizes apoptotic cells for phagocytic removal via receptors of the Mer/Axl/Tyro3 tyrosine kinase family,[33,34] and a Dex-induced upregulation of MerTK expression has been described.[25,26] In our initial qRT-PCR screen, we observed a slight, yet statistically not significant, upregulation of MerTK expression in peripheral blood monocytes of patients under high-dose prednisone treatment. Monocytes and not macrophages were employed in this screen; this might account for the fact that MerTK was not identified as a Dex-upregulated target gene. Moreover, for the functional characterization of the involvement of Protein S and MerTK, McColl *et al.*[25] and Zahuczky *et al.*[26] employed macrophages that had been differentiated from peripheral monocytes in the presence of Dex, whereas in our study Dex was applied to finally differentiate macrophages. It is conceivable that Dex modulates the differentiation process itself and favours the maturation of a different macrophage phenotype, which relies on other engulfment receptors than those macrophages employed in our study. In addition, McColl *et al.* analyzed the phagocytosis of apoptotic cells in the presence of serum. We observed the GC-mediated enhancement of efferocytosis in the presence but also in the absence of serum. In the latter condition, Protein S and other serum-derived opsonins are unlikely to be involved. Thus, the results shown in the present study together with the results from McColl *et al.*[25] and Zahuczky *et al.*[26] suggest a scenario, in which protein S and MerTK account for the Dex-mediated enhancement of apoptotic cell clearance under conditions where serum proteins are abundant and where macrophages rely on the Protein S-MerTK axis. MFG-E8, in contrast, might govern the Dex-dependent phagocytosis promotion in the absence or under low concentrations of Protein S. Here, macrophages utilize opsonins, which they either produce autonomously, or which are provided by neighboring cells in the respective tissues.[35] Our *in vivo* model of irradiation-induced thymus atrophy clearly argues for an involvement of MFG-E8 in this context, and further analyses have to clarify in which tissues or organs Protein S and MerTK are required for apoptotic cell clearance.

Mechanistically, our results reveal a direct, GR-dependent transactivation of MFG-E8 mRNA expression mediated by a full GRE motif at position -667 and two GRE half-sites at positions -449 and -251 within the human MFG-E8 promoter of certain myeloid cells. As the GR is rather ubiquitously expressed, the cell-type specificity of Dex-dependent MFG-E8 induction might be coupled to transcriptional co-activators, which are only expressed in myeloid subpopulations, or it is plausible to assume that Dex-dependent MFG-E8 induction requires some kind of basal transcriptional activity of the MFG-E8 promoter or open chromatin, which is specifically

found in the respective cellular subsets. Further studies are required to elucidate this issue in greater detail. Apart from direct transcriptional activation, we have observed a stabilization of MFG-E8 mRNA in response to Dex treatment resulting in an ~2-fold prolonged half-life of MFG-E8 mRNA, which presumably also contributes to enhanced MFG-E8 protein expression. A similar Dex-mediated stabilization of mRNA has also been reported for other genes, such as fatty acid synthase.[36] AU-rich elements (AREs) in the 3′-untranslated region (UTR) are known to regulate mRNA stability, and the expression of the ARE-binding protein, tristetraprolin, which promotes mRNA deadenylation and destabilization, has been shown to be inhibited in Dex-treated macrophages.[37,38] The interference with tristetraprolin-mediated mRNA destabilization is, thus, likely to be responsible for the Dex-dependent prolongation of MFG-E8 mRNA half-life, as an ARE is located in the MFG-E8 3′UTR at position +1857.

To date, the anti-phlogistic effects of GCs are consentaneously considered to be caused by the GR-mediated transrepression of pro-inflammatory cytokines, like IL-1β, IL-2, IL-6, IL-8, IL-12, IFNγ, CCL2 and TNF, due to the inhibition of NF-κB-, cAMP response element binding-, interferon regulatory factor3-, nuclear factor of activated T cells- and activator protein-1 activity.[19] So far, only a few anti-inflammatory mediators, like IL-10, Anx A1 and IL-1 receptor antagonist, have been shown to be GR-dependently induced via transactivation.[27] Furthermore, various undesirable side effects (insulin resistance, osteoporosis, glaucoma, skin atrophy and disturbed wound healing) often limiting the applicability of long-term GC administration have been attributed to GR-mediated transactivation of diverse genes.[20] Consequently, in the recent years intense scientific effort has been invested into the search for new, selective GR agonists (SEGRAs), which dissect favorable GR-dependent transrepression from unwanted GR-dependent transactivation.[39,40] Here, we present *in vitro* and *in vivo* evidence that the GC-mediated transactivation of MFG-E8 expression and the concomitantly enhanced non-phlogistic phagocytic uptake of apoptotic cells constitute a novel aspect of the anti-inflammatory action of GCs. This might be of particular importance in the therapeutic context of diseases associated with an impaired clearance of apoptotic cells, like SLE. Thus, future studies have to reveal whether SEGRAs do address this issue and if other modulators of MFG-E8 transactivation might be of therapeutic value for systemic autoimmune diseases.

Materials and Methods

Patients. Patients were recruited from our outpatient clinic and met the diagnostic criteria of the American College of Rheumatology. Healthy volunteers served as controls. An informed consent was obtained from all blood donors and the study received the final approval from the ethics committee of the University Hospital Erlangen. Available data regarding demographics, diagnosis and therapy are summarized in Supplementary Table 1.

Mice. Generation of MFG-E8$^{-/-}$ mice was described previously.[16] All animal experiments were approved by the government of Mittelfranken. Mice were housed in the animal facility of the University of Erlangen-Nuremberg.

Irradiation-induced thymus atrophy. C57BL/6 mice and MFG-E8$^{-/-}$ mice were treated with 1 mg/kg/week Dex intraperitoneally for 1 week (applied in seven daily doses). Then, mice were irradiated with 0.5 Gy, killed after 8 h and subjected to thymectomy. Thymus atrophy was determined as the percentage of residual thymus mass in comparison with the non-irradiated controls.

For histological examination, explanted thymi were fixed overnight in 4% paraformaldehyde and embedded in paraffin. Five-micrometer-thick dewaxed and permeablized sections were used for fluorescence staining employing TUNEL–FITC detection of dying cells with DNA strand breaks according to the manufacturer's instructions (Roche Applied Science, Penzberg Germany), and DAPI staining (Sigma, Deisenhofen, Germany) was performed for the visualization of all nuclei. Histological sections were examined at ×2 and ×10 magnification using a fluorescence microscope (Nikon, Berlin, Germany) equipped with a digital camera. Pictures were taken with identical camera settings.

For subsequent FACS analyses of different types of cell death, explanted thymi were mechanically disrupted. Flushed-out cells were subjected to FSC/SSC FACS analyses or to 6-parameter FACS staining on the basis of cellular granularity (SSC) and shrinkage (FSC), PS exposure (Annexin A5-FITC), ion selectivity of the plasma membrane (propidium iodide), mitochondrial membrane potential (DiIC$_1$(5)) and DNA content (Hoechst 33342). The percentage of total dead cells, apoptotic, primary and secondary necrotic cells was determined as previously described.[41] Briefly, cells were classified as follows:

Viable cells: high FSC, low SSC, low Annexin A5, low PI and high Hoechst 33342.

Apoptotic cells: high/low FSC, low/high SSC, high Annexin A5, low PI, high/low DiIC$_1$(5) and high Hoechst 33342.

Secondary necrotic cells: low FSC, high SSC, high Annexin A5, intermediate PI, low DiIC$_1$(5) and high/intermediate Hoechst 33342.

Primary necrotic: low FSC, high SSC, high Annexin A5, high PI, low DiIC$_1$(5) and high Hoechst 33342.

Cells, reagents and plasmid constructs. THP-1 and U937 cells obtained from ATCC were cultured in RPMI-1640 supplemented with 10% heat-inactivated fetal calf serum, 100 units of penicillin/ml, 0.1 mg streptomycin/ml and 10 mM HEPES (all from Invitrogen Life Technologies, Karlsruhe, Germany). Differentiation into macrophages was carried out with 10 nM phorbol–myristyl–acetate (PMA, Sigma) for 16 h followed by further cultivation for 48 h in PMA-free medium.

Human PBMCs were prepared from heparinized blood by Ficoll density gradient centrifugation (Ficoll-Paque 1.077 g/ml, GE Healthcare, Freiburg, Germany). Primary human monocytes were positively selected from PBMCs with anti-CD14 magnetic beads (Miltenyi, Bergisch Gladbach, Germany) according to the manufacturer's recommendation. Monocyte-derived macrophages were generated by differentiation of peripheral monocytes with 20 ng/ml M-CSF or GM-CSF (R&D Systems, Heidelberg, Germany) in macrophage medium (Invitrogen Life Technologies) supplemented with 5% autologous serum for 7 days.

PHA-stimulated PBMCs (PHA lymphoblasts) were prepared by cultivating human PBMCs for 7 days in RPMI-1640 supplemented with 10% heat-inactivated fetal calf serum, 100 units of penicillin/ml, 0.1 mg streptomycin/ml, 10 mM HEPES and 0.5 μg/ml PHA (Biochrom, Berlin, Germany).

Thioglycollate-elicited macrophages were isolated from C57BL/6 and MFG-E8$^{-/-}$ mice by peritoneal lavage of mice that had been injected with 1 ml of 2% thioglycollate in PBS 3 days before.

Primary human foreskin fibroblasts were prepared as described previously[42] and cultivated in DMEM supplemented with 10% heat-inactivated fetal calf serum, 100 units of penicillin/ml and 0.1 mg streptomycin/ml. The same medium was used for murine NIH3T3 fibroblasts expressing $\alpha_v\beta_3$ integrin, which were described previously.[12]

Human neutrophils were obtained by double-Ficoll gradient purification (Histopaque 1.119 g/ml, Sigma, and Ficoll-Paque 1.077 g/ml, GE Healthcare) and were used 24 h after preparation, when they had undergone spontaneous apoptosis. In this stage, ~75% were apoptotic (Annexin V-positive and PI-negative), whereas <10% were secondary necrotic (Annexin V-positive and PI-positive).

Apoptotic THP-1 prey cells were generated by UV-C irradiation (10 mJ/cm^2). At 12 h post irradiation, when prey cells were fed to macrophages, ~70% were apoptotic (Annexin V-positive and PI-negative), whereas <10% were secondary necrotic (Annexin V-positive and PI-positive).

Thymocytes of C57BL/6 mice were stimulated to undergo apoptosis by UV-B irradiation (270 mJ/cm^2) followed by *in vitro* culture for 16 h. At that time, ~60% of the cells were apoptotic (Annexin V-positive and PI-negative), whereas <20% were secondary necrotic (Annexin V-positive and PI-positive).

Secondary necrotic fragments were generated by digestion of heat-treated human peripheral blood lymphocytes by serum DNase I and C1q followed by PI staining as described previously.[43]

Dex was purchased from Merck Biosciences (Darmstadt, Germany). ActD and CHX were from Sigma and Carl Roth (Karlsruhe, Germany), respectively. PKH67 and PKH26 were obtained from Sigma, CFSE from Invitrogen and RU486 was from Merck Biosciences. Polybead carboxylate red-dyed microspheres (6 μm) were purchased from Polysciences (Eppleheim, Germany).

Monoclonal anti-MFG-E8 antibodies (mouse mAB clone 1-H3, hamster mAB clone 2-8E4A and hamster mAB clone 2-11B4A) and recombinant human MFG-E8 were described previously.[44]

The promoter region of human MFG-E8 (nt -950 to $+60$) was amplified by PCR from genomic THP-1 cell DNA and cloned into the BglII/HindIII site of pGL3 Basic (Promega, Heidelberg, Germany) according to standard procedures. For the generation of the deletion mutants, the full-length construct was digested with different combinations of BglII/AflII (nt -508 to $+60$), BalI/HindIII (nt -950 to -80) or AflII/BalI (nt -950 to $+60$, del -508 to -80) (see Figure 3e), the cohesive ends were filled up with Klenow enzyme and the plasmids were religated.

siRNA-mediated MFG-E8 knockdown. Chemically modified siRNA oligonucleotides (stealth RNAi) were purchased from Invitrogen. The following oligonucleotides were used: MFG-E8 nt63: 5′-CGUCGCCCUGGAUAUCUGUUC CAAA-3′, scramble: 5′-CGUUCCCUAGGUCUACUUGCGCAAA-3′. Electroporation of 5×10^6 THP-1 cells with 2 μM siRNA oligo in 500 μl OptiMEM (Invitrogen) was performed as described[45,46] At 24 h before PKH67 staining and PMA-induced differentiation into macrophages, electroporation of 5×10^6 primary monocytes with 2 μM siRNA oligo in 500 μl OptiMEM (Invitrogen) was performed as described[45,46] on d0, d1 and d4 after preparation before PKH67 staining and differentiation with 20 ng/ml M-CSF into macrophages on d1. Dex treatment was applied on d4 for 24 h and all other assays (qRT-PCR and phagocytosis assays) were performed on d5.

Phagocytosis assay. Phagocytosis assays were performed as described previously.[47,48] Briefly, green (PKH67)-stained, PMA-differentiated THP-1 macrophages (1×10^5 cells/well in a 24-well plate) were fed with different ratios of red-stained prey cells (apoptotic THP-1 cells were stained with PKH26 and secondary necrotic fragments were stained with PI) or red-dyed microspheres (6 μm Polybead carboxylate red-dyed microspheres) in a final volume of 500 μl serum-free medium and incubated at 37 °C for 2 h. Subsequently, cells were harvested by trypsinization and analyzed by flow cytometry. Phagocytosis was determined as the percentage of double-positive macrophages.

Thioglycollate-elicited macrophages were seeded in polystyrene tubes (2.5×10^5 cells/tube) and were fed with apoptotic, CFSE-stained thymocytes (ratio 1 : 1) at 37 °C for 8 h. Cells were collected in cold PBS supplemented with 5 mM EDTA, stained with F4/80-PE-Cy5 antibody and analyzed by flow cytometry. Phagocytosis was measured as the product of the percentage of double-positive macrophages and the mean intensity of prey cell fluorescence per engulfing macrophage, and was finally normalized on the mean of the corresponding untreated control cell population.

Quantitative real-time PCR. QRT-PCR analysis was performed using the ABI Prism 7000 Sequence Detection System (Applied Biosystems, Foster City, CA, USA) and Maxima qPCR Mastermix (Fermentas, St. Leon-Rot, Germany) as described.[49–51] The following primers and probes were used (MWG Biotech, Ebersberg, Germany): human MFG-E8 forward 5′-GCACTCTGCGCTTTGAGC TA-3′, human MFG-E8 reverse 5′-TTGTCAGGGATGCTGTTATTCTTC-3′; human Anx A1 forward 5′-GCCCCTATCCTACCTTCAATCC-3′, human Anx A1 reverse 5′-CATCCACACCTTTAACCATTATGG-3′; human Del-1 forward 5′-CAGGCGAAT TTATGGGAAGAAA-3′, human Del-1 reverse 5′-TGCTGGTTTGATATAATTCCAC CTT-3′; mouse MFG-E8 forward 5′-AAAGCTGTACCCTGTTTCGTGC-3′, mouse MFG-E8 reverse 5′-GGAGGCTGACATCTGGCTGT-3′; human/mouse 18 S rRNA forward 5′-CGGCTACCACATCCAAGGAA-3′, human/mouse 18 S rRNA reverse 5′-GCTGGAATTACCGCGGCT-3′, human/mouse 18 S rRNA probe JOE-5′-TGCT GGCACCAGACTTGCCCTC-3′-TAMRA.

Total RNA from $\sim 2 \times 10^6$ cells was extracted with the NucleoSpin RNA II-Kit (Macherey and Nagel, Dueren, Germany). One microgram of total RNA was reverse transcribed with 200 U Superscript RT II reverse transcriptase (Invitrogen) in the presence of 50 μM random hexamers (GE Healthcare), 400 μM dNTPs (Promega) and 1.6 U/μl RNAsIn (Invitrogen) in a final volume of 25 μl. Resulting cDNA (40–80 ng) were applied to the following qRT-PCR analyses (20 μl final volume) and amplified in the presence of 300 nM primers (SYBR Green PCR) or 50 nM primers and 200 nM probe (Taqman PCR), respectively, with the standard temperature profile (2 min 50 °C, 10 min 95 °C, 40 × (15 s 95 °C, 1 min 60 °C)). Relative quantification was performed employing the standard curve method and the results were normalized on 18 S rRNA. Calibration is indicated in the figure legends.

SDS-PAGE and western blot analyses. For immunoblot detection of MFG-E8 in cellular lysates, secretion was blocked by addition of 10 μg/ml Brefeldin A (Sigma) during the last 4 h of incubation. Non-reducing gradient SDS-PAGE and western blot analyses of whole cell lysates were performed as described previously[46,52] with 100 μg protein extract per lane and monoclonal mouse antibodies against human MFG-E8 (clone 1-H3)[44] and vinculin (Sigma) followed by ECL detection (GE Healthcare).

MFG-E8 ELISA. MFG-E8 protein levels were quantitfied by ELISA of cell-free culture supernatants and cellular lysates according to the manufacturer's instructions (USCN Life Science Inc., Houston, TX, USA). The measured protein levels are displayed as pg MFG-E8 per 1 Mio. cells.

Luciferase activity assay. PMA-differentiated THP-1 macrophages (1×10^6 cells per well in a 6-well plate) were transfected with 2 μg of the different MFG-E8 promoter constructs and FuGENE HD (Roche, Penzberg, Germany) for 5 h according to the manufacturer's instructions. Subsequently, cells were stimulated with 0–1000 nM Dex for 18 h. Luciferase activity in cellular lysates was measured with a Berthold Lumat 9507 luminometer (Berthold Technologies, Bad Wildbad, Germany) as described.[53] Briefly, 1×10^6 cells were lysed in 100 μl lysis buffer (25 mM Tris-HCl pH 7.8, 2 mM EDTA, 10% glycerol, 1% Triton X-100, 2 mM DTT) and assayed for luciferase activity in 15 mM glycyl–glycine, 10 mM $MgCl_2$, 3 mM ATP and 50 μM D-luciferin (measuring time 10 s). For every construct, the results were normalized on the corresponding untreated control cell lysate.

Conflict of Interest

The authors declare no conflict of interest.

Acknowledgements. We thank Christian Sinzger and Johanna Reichel, who kindly provided primary human foreskin fibroblasts. This work was supported by the DFG He 4490/3-1 (MH), SFB 643 (MH), SFB 685 (KL and SW), SFB 914 (KL), LMU excellent (KL), Universität Bayern e.V. (KL), the Interdisciplinary Center for Clinical Research (IZKF) at the University Hospital of the University of Erlangen-Nuremberg (MH) and the Programme Alban of the European Commission, no. E04D047956VE (MH).

Author contributions

KL, SW, CB and MH conceived and designed experiments. HY and SN provided MFG-E8 $^{-/-}$ mice, purified MFG-E8, and NIH3T3 fibroblasts expressing the MFG-E8 receptor $\alpha_v\beta_3$ integrin. KL, HK, UK, KS, LEM, HY, GK and SU performed experiments and analyzed the data. KL and MH wrote the manuscript, and all authors discussed the results and commented on the manuscript.

1. Wickman G, Julian L, Olson MF. How apoptotic cells aid in the removal of their own cold dead bodies. *Cell Death Differ* 2012; **19**: 735–742.
2. Ravichandran KS. Beginnings of a good apoptotic meal: the find-me and eat-me signaling pathways. *Immunity* 2011; **35**: 445–455.
3. Poon IK, Hulett MD, Parish CR. Molecular mechanisms of late apoptotic/necrotic cell clearance. *Cell Death Differ* 2010; **17**: 381–397.
4. Munoz LE, Lauber K, Schiller M, Manfredi AA, Herrmann M. The role of defective clearance of apoptotic cells in systemic autoimmunity. *Nat Rev Rheumatol* 2010; **6**: 280–289.
5. Gaipl US, Munoz LE, Grossmayer G, Lauber K, Franz S, Sarter K *et al.* Clearance deficiency and systemic lupus erythematosus (SLE). *J Autoimmun* 2007; **28**: 114–121.
6. Miyanishi M, Tada K, Koike M, Uchiyama Y, Kitamura T, Nagata S. Identification of Tim4 as a phosphatidylserine receptor. *Nature* 2007; **450**: 435–439.
7. Park D, Tosello-Trampont AC, Elliott MR, Lu M, Haney LB, Ma Z *et al.* BAI1 is an engulfment receptor for apoptotic cells upstream of the ELMO/Dock180/Rac module. *Nature* 2007; **450**: 430–434.
8. Park SY, Jung MY, Kim HJ, Lee SJ, Kim SY, Lee BH *et al.* Rapid cell corpse clearance by stabilin-2, a membrane phosphatidylserine receptor. *Cell Death Differ* 2008; **15**: 192–201.

9. Nakayama M, Akiba H, Takeda K, Kojima Y, Hashiguchi M, Azuma M *et al.* Tim-3 mediates phagocytosis of apoptotic cells and cross-presentation. *Blood* 2009; **113**: 3821–3830.
10. Schutters K, Kusters DH, Chatrou ML, Montero-Melendez T, Donners M, Deckers NM *et al.* Cell surface-expressed phosphatidylserine as therapeutic target to enhance phagocytosis of apoptotic cells. *Cell Death Differ* 2013; **20**: 49–56.
11. Wu Y, Tibrewal N, Birge RB. Phosphatidylserine recognition by phagocytes: a view to a kill. *Trends Cell Biol* 2006; **16**: 189–197.
12. Hanayama R, Tanaka M, Miwa K, Shinohara A, Iwamatsu A, Nagata S. Identification of a factor that links apoptotic cells to phagocytes. *Nature* 2002; **417**: 182–187.
13. Akakura S, Singh S, Spataro M, Akakura R, Kim JI, Albert ML *et al.* The opsonin MFG-E8 is a ligand for the alphavbeta5 integrin and triggers DOCK180-dependent Rac1 activation for the phagocytosis of apoptotic cells. *Exp Cell Res* 2004; **292**: 403–416.
14. Nandrot EF, Anand M, Almeida D, Atabai K, Sheppard D, Finnemann SC. Essential role for MFG-E8 as ligand for alphavbeta5 integrin in diurnal retinal phagocytosis. *Proc Natl Acad Sci USA* 2007; **104**: 12005–12010.
15. Kranich J, Krautler NJ, Falsig J, Ballmer B, Li S, Hutter G *et al.* Engulfment of cerebral apoptotic bodies controls the course of prion disease in a mouse strain-dependent manner. *J Exp Med* 2010; **207**: 2271–2281.
16. Hanayama R, Tanaka M, Miyasaka K, Aozasa K, Koike M, Uchiyama Y *et al.* Autoimmune disease and impaired uptake of apoptotic cells in MFG-E8-deficient mice. *Science* 2004; **304**: 1147–1150.
17. Peng Y, Elkon KB. Autoimmunity in MFG-E8-deficient mice is associated with altered trafficking and enhanced cross-presentation of apoptotic cell antigens. *J Clin Invest* 2011; **121**: 2221–2241.
18. Herrmann M, Voll RE, Zoller OM, Hagenhofer M, Ponner BB, Kalden JR. Impaired phagocytosis of apoptotic cell material by monocyte-derived macrophages from patients with systemic lupus erythematosus. *Arthritis Rheum* 1998; **41**: 1241–1250.
19. De Bosscher K, Haegeman G. Minireview: latest perspectives on antiinflammatory actions of glucocorticoids. *Mol Endocrinol* 2009; **23**: 281–291.
20. Schacke H, Docke WD, Asadullah K. Mechanisms involved in the side effects of glucocorticoids. *Pharmacol Ther* 2002; **96**: 23–43.
21. Hanayama R, Tanaka M, Miwa K, Nagata S. Expression of developmental endothelial locus-1 in a subset of macrophages for engulfment of apoptotic cells. *J Immunol* 2004; **172**: 3876–3882.
22. Perretti M, D'Acquisto F. Annexin A1 and glucocorticoids as effectors of the resolution of inflammation. *Nat Rev Immunol* 2009; **9**: 62–70.
23. Jinushi M, Nakazaki Y, Dougan M, Carrasco DR, Mihm M, Dranoff G. MFG-E8-mediated uptake of apoptotic cells by APCs links the pro- and antiinflammatory activities of GM-CSF. *J Clin Invest* 2007; **117**: 1902–1913.
24. Liu Y, Cousin JM, Hughes J, Van Damme J, Seckl JR, Haslett C *et al.* Glucocorticoids promote nonphlogistic phagocytosis of apoptotic leukocytes. *J Immunol* 1999; **162**: 3639–3646.
25. McColl A, Bournazos S, Franz S, Perretti M, Morgan BP, Haslett C *et al.* Glucocorticoids induce protein S-dependent phagocytosis of apoptotic neutrophils by human macrophages. *J Immunol* 2009; **183**: 2167–2175.
26. Zahuczky G, Kristof E, Majai G, Fesus L. Differentiation and glucocorticoid regulated apopto-phagocytic gene expression patterns in human macrophages. Role of Mertk in enhanced phagocytosis. *PLoS One* 2011; **6**: e21349.
27. Newton R, Holden NS. Separating transrepression and transactivation: a distressing divorce for the glucocorticoid receptor? *Mol Pharmacol* 2007; **72**: 799–809.
28. Rhen T, Cidlowski JA. Antiinflammatory action of glucocorticoids–new mechanisms for old drugs. *N Engl J Med* 2005; **353**: 1711–1723.
29. Giles KM, Ross K, Rossi AG, Hotchin NA, Haslett C, Dransfield I. Glucocorticoid augmentation of macrophage capacity for phagocytosis of apoptotic cells is associated with reduced p130Cas expression, loss of paxillin/pyk2 phosphorylation, and high levels of active Rac. *J Immunol* 2001; **167**: 976–986.
30. Maderna P, Yona S, Perretti M, Godson C. Modulation of phagocytosis of apoptotic neutrophils by supernatant from dexamethasone-treated macrophages and annexin-derived peptide Ac(2-26). *J Immunol* 2005; **174**: 3727–3733.
31. Gebicke-Haerter PJ, Schobert A, Dieter P, Honegger P, Hertting G. Regulation and glucocorticoid-independent induction of lipocortin I in cultured astrocytes. *J Neurochem* 1991; **57**: 175–183.
32. Donnelly SR, Moss SE. Functional analysis of the human annexin I and VI gene promoters. *Biochem J.* 1998; **332**(Pt 3): 681–687.
33. Anderson HA, Maylock CA, Williams JA, Paweletz CP, Shu H, Shacter E. Serum-derived protein S binds to phosphatidylserine and stimulates the phagocytosis of apoptotic cells. *Nat Immunol* 2003; **4**: 87–91.
34. Lemke G, Rothlin CV. Immunobiology of the TAM receptors. *Nat Rev Immunol* 2008; **8**: 327–336.
35. Kranich J, Krautler NJ, Heinen E, Polymenidou M, Bridel C, Schildknecht A *et al.* Follicular dendritic cells control engulfment of apoptotic bodies by secreting Mfge8. *J Exp Med* 2008; **205**: 1293–1302.
36. Xu ZX, Rooney SA. Glucocorticoids increase fatty-acid synthase mRNA stability in fetal rat lung. *Am J Physiol* 1997; **272**(5 Pt 1): L860–L864.
37. Chen CY, Shyu AB. AU-rich elements: characterization and importance in mRNA degradation. *Trends Biochem Sci* 1995; **20**: 465–470.
38. Jalonen U, Lahti A, Korhonen R, Kankaanranta H, Moilanen E. Inhibition of tristetraprolin expression by dexamethasone in activated macrophages. *Biochem Pharmacol* 2005; **69**: 733–740.
39. McMaster A, Ray DW. Drug insight: selective agonists and antagonists of the glucocorticoid receptor. *Nat Clin Pract Endocrinol Metab* 2008; **4**: 91–101.
40. De Bosscher K. Selective glucocorticoid receptor modulators. *J Steroid Biochem Mol Biol* 2010; **120**: 96–104.
41. Munoz LE, Maueroder C, Chaurio R, Berens C, Herrmann M, Janko C. Colourful death: six-parameter classification of cell death by flow cytometry-dead cells tell tales. *Autoimmunity* 2013; e-pub ahead of print 12 February 2013; doi:10.3109/08916934.2012.755960.
42. Jiang XJ, Adler B, Sampaio KL, Digel M, Jahn G, Ettischer N *et al.* UL74 of human cytomegalovirus contributes to virus release by promoting secondary envelopment of virions. *J Virol* 2008; **82**: 2802–2812.
43. Gaipl US, Beyer TD, Heyder P, Kuenkele S, Bottcher A, Voll RE *et al.* Cooperation between C1q and DNase I in the clearance of necrotic cell-derived chromatin. *Arthritis Rheum* 2004; **50**: 640–649.
44. Yamaguchi H, Takagi J, Miyamae T, Yokota S, Fujimoto T, Nakamura S *et al.* Milk fat globule EGF factor 8 in the serum of human patients of systemic lupus erythematosus. *J Leukoc Biol* 2008; **83**: 1300–1307.
45. Peter C, Waibel M, Radu CG, Yang LV, Witte ON, Schulze-Osthoff K *et al.* Migration to apoptotic "find-me" signals is mediated via the phagocyte receptor G2A. *J Biol Chem* 2008; **283**: 5296–5305.
46. Peter C, Waibel M, Keppeler H, Lehmann R, Xu G, Halama A *et al.* Release of lysophospholipid 'find-me' signals during apoptosis requires the ATP-binding cassette transporter A1. *Autoimmunity* 2012; **45**: 568–573.
47. Blume KE, Soeroes S, Waibel M, Keppeler H, Wesselborg S, Herrmann M *et al.* Cell surface externalization of annexin A1 as a failsafe mechanism preventing inflammatory responses during secondary necrosis. *J Immunol* 2009; **183**: 8138–8147.
48. Rosenwald M, Koppe U, Keppeler H, Sauer G, Hennel R, Ernst A *et al.* Serum-derived plasminogen is activated by apoptotic cells and promotes their phagocytic clearance. *J Immunol* 2012; **189**: 5722–5728.
49. Andre MC, Gille C, Glemser P, Woiterski J, Hsu HY, Spring B *et al.* Bacterial reprogramming of PBMCs impairs monocyte phagocytosis and modulates adaptive T cell responses. *J Leukoc Biol* 2012; **91**: 977–989.
50. Harre U, Keppeler H, Ipseiz N, Derer A, Poller K, Aigner M *et al.* Moonlighting osteoclasts as undertakers of apoptotic cells. *Autoimmunity* 2012; **45**: 612–619.
51. Wagner BJ, Lindau D, Ripper D, Stierhof YD, Glatzle J, Witte M *et al.* Phagocytosis of dying tumor cells by human peritoneal mesothelial cells. *J Cell Sci* 2011; **124**(Pt 10): 1644–1654.
52. Blume KE, Soeroes S, Keppeler H, Stevanovic S, Kretschmer D, Rautenberg M *et al.* Cleavage of annexin A1 by ADAM10 during secondary necrosis generates a monocytic "find-me" signal. *J Immunol* 2012; **188**: 135–145.
53. Lindemann RK, Braig M, Ballschmieter P, Guise TA, Nordheim A, Dittmer J. Protein kinase Calpha regulates Ets1 transcriptional activity in invasive breast cancer cells. *Int J Oncol* 2003; **22**: 799–805.

Supplementary Information accompanies this paper on Cell Death and Differentiation website (http://www.nature.com/cdd)